Dalton Transactions

PAPER

View Article Online
View Journal | View Issue

Cite this: *Dalton Trans.*, 2015, **44**, 15334

Porous frameworks constructed by non-covalent linking of substitution-inert metal complexes†

Takahiro Itoh,[a,b] Mio Kondo,*[a,b,c,d] Hirotoshi Sakamoto,[e] Kaori Wakabayashi,[a] Mari Kanaike,[a] Kenichiro Itami[e,f,g] and Shigeyuki Masaoka*[a,b,d]

Received 30th April 2015,
Accepted 17th July 2015

DOI: 10.1039/c5dt01620g

www.rsc.org/dalton

The incorporation of active sites into metal–organic frameworks (MOFs) or porous coordination polymers (PCPs) is an attractive way to functionalise these materials. However, the methodology to organise substitution-inert metal-based secondary building units (SBUs) with active sites into MOFs or PCPs *via* coordination driven self-assembly is severely limited. In this study, we successfully assembled substitution-inert paddle-wheel Rh(II) dimers to afford three novel porous frameworks, $Rh_2(ppeb)_4(THF)_2$ (**1-THF**), $Rh_2(ppeb)_4$(3-pentanone)$_2$ (**1-PN**) and $Rh_2(ppeb)_4$(1-adamantylamine)$_2$ (**1-AD**) (ppeb = 4-[(perfluorophenyl)ethynyl]benzoate), by using non-covalent interactions. Multipoint arene–perfluoroarene (Ar–Ar^F) interactions, which allow the unidirectional face-to-face interaction mode of aromatic rings, were used to assemble the substitution-inert paddle-wheel Rh(II) dimers. The obtained frameworks were structurally characterisation by single crystal X-ray diffraction, and it is found that all structures exhibited a one-dimensional channel with active axial sites exposed to the pores. The porous properties of the obtained frameworks were also investigated by thermogravimetric analysis, gas adsorption and powder X-ray diffraction measurements. Moreover, the ligand substitution reaction at the active axial sites was examined at the crystalline state and the flexible structural transformation with the change of channel shapes and sizes was observed.

Introduction

Metal–organic frameworks (MOFs) or porous coordination polymers (PCPs)[1,2] are crystalline materials composed of inorganic building units and organic linkers and have attracted considerable attention as new types of porous materials. In particular, MOFs or PCPs with open metal sites are of interest because these sites can strongly interact with adsorbed molecules to afford specific functionalisation of the pore surfaces for adsorption/separation,[3] heterogeneous catalysis,[4] and sensing.[5] One of the most straightforward strategies to construct such materials is to embed open metal sites on secondary building units (SBUs) of the framework.[6] The Rh(II) paddle-wheel complex, which is composed of four substitution-inert carboxylate ligands and two substitution-labile axial ligands, would be an attractive SBU with D_{4h} symmetry because the porous frameworks constructed are expected to show high stability arising from the substitution-inert carboxylate ligands and the high reactivity of the substitution-labile axial sites known as active centres for many catalytic reactions.[7] However, it is hard to construct MOFs or PCPs by linking substitution-inert metal-based SBUs *via* covalent linkers (Scheme 1a) because the covalent linking of these SBUs often prevents the formation of single crystalline materials.[8] Although there are many reports on single crystal structures of MOFs and PCPs consisting of substitution-labile SBUs with active sites (*e.g.*, HKUST-1,[6a] MOF-74,[6b] and so on[9]), to the best of our knowledge, no single crystal structures of MOFs or PCPs constructed by substitution-inert SBUs with those sites have been reported so far.

Here, we show an effective approach to construct a porous framework based on substitution-inert SBUs with active sites. Recently, many reports have proven that non-covalent interactions (*e.g.*, hydrogen bonds,[10] π–π interactions,[11] combi-

[a]*Department of Life and Coordination-Complex Molecular Science, Institute for Molecular Science, 5-1 Higashiyama, Myodaiji, Okazaki, Aichi 444-8787, Japan. E-mail: mio@ims.ac.jp, masaoka@ims.ac.jp*
[b]*SOKENDAI [The Graduate University for Advanced Studies], Shonan Village, Hayama, Kanagawa 240-0193, Japan*
[c]*ACT-C, Japan Science and Technology Agency (JST), 4-1-8 Honcho, Kawaguchi, Saitama 332-0012, Japan*
[d]*Research Center of Integrative Molecular Systems (CIMoS), Institute for Molecular Science, 38 Nishigo-naka, Myodaiji, Okazaki, Aichi 444-8585, Japan*
[e]*JST, ERATO, Itami Molecular Nanocarbon Project, Chikusa, Nagoya 464-8602, Japan*
[f]*Graduate School of Science, Nagoya University, Chikusa, Nagoya 464-8602, Japan*
[g]*Institute of Transformative Bio-Molecules (WPI-ITbM), Nagoya University, Nagoya 464-8602, Japan*

†Electronic supplementary information (ESI) available: Figures of CO_2 or N_2 sorption isotherms, PXRD patterns. CCDC 1049445–1049447. For ESI and crystallographic data in CIF or other electronic format see DOI: 10.1039/c5dt01620g

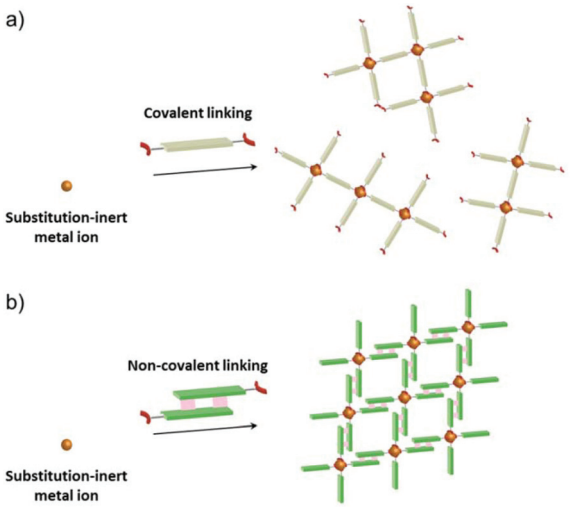

Scheme 1 Schematic illustration of the self-assembly of substitution-inert SBUs *via* (a) covalent linking and (b) non-covalent linking.

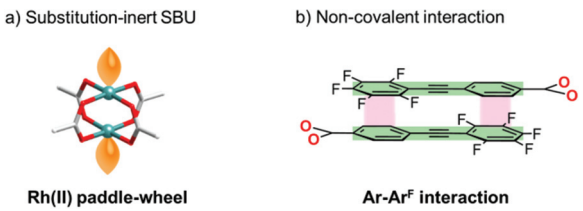

Scheme 2 Schematic illustration of (a) substitution inert SBU and (b) non-covalent interaction employed in this study.

nation of hydrogen bonds and π–π interactions,[12] and van der Waals interactions[13]) can be promising tools for the construction of porous materials. In comparison with covalent linking, these interactions can work under ambient conditions to afford a comparable well-defined framework. A key to our success is the usage of this "non-covalent" interaction (Scheme 1b) for the self-assembly of Rh(II) paddle-wheel dimers (Scheme 2a). As a module for non-covalent linking, a monocarboxylate ligand with multipoint arene–perfluoroarene[14] (Ar–Ar^F) interaction sites was designed (Scheme 2b). As we have previously reported this interaction enables the unidirectional face-to-face interaction mode of aromatic rings to work dominantly, and the controlled self-assembly of molecules can be achieved.[15]

Experimental

General methods

All solvents and reagents were of the highest quality available and used as received except for diethylamine and triethylamine. Diethylamine and triethylamine were dried by refluxing over KOH, distilled under argon, and degassed with a freeze-and-pump thaw. 4-[(Perfluorophenyl)ethynyl]benzoic acid (Hppeb) and $Na_4[Rh_2(CO_3)_4]$ were prepared by using the literature methods.[15,16] All syntheses were performed under an atmosphere of dry nitrogen or dry argon unless otherwise indicated. Elemental analysis was carried out on a J-SCIENCE LAB MICRO CORDER JM10 elemental analyser. The ^{1}H NMR spectrum was acquired on a JEOL JNM-LA500 spectrometer, where chemical shifts in DMF-d_7 were referenced to internal tetramethylsilane. The ^{19}F NMR spectrum was acquired on a JEOL JNM-LA500 spectrometer, where chemical shifts in DMF-d_7 were referenced to external trifluorotoluene. Thermogravimetric analyses (TGA) were carried out with a SHIMADZU DTG-60 under a nitrogen atmosphere. TGA profiles of **1-THF**, **1-PN** and **1-AD** were measured at a heating rate of 20 K min^{-1}. Fourier transformed infrared spectra were recorded on a Perkin-Elmer Spectrum 100 FT-IR spectrometer equipped with an ATR (Attenuated Total Reflectance) accessory.

Synthetic procedures

Synthesis of $Rh_2(ppeb)_4(Et_2O)_2$. $Na_4[Rh_2(CO_3)_4]\cdot 3H_2O$ (59 mg, 0.10 mmol) and Hppeb (250 mg, 0.80 mmol) in 40 ml of dimethylacetamide/H_2O mixed solvents were stirred for 8 h at 100 °C. After evaporation of the solvent, the residue was washed with water and dissolved in Et_2O and subsequently purified by column chromatography using neutral alumina (Et_2O as eluent). The yield of $[Rh_2(ppeb)_4]$ was 44 mg (27% based on $Na_4[Rh_2(CO_3)_4]\cdot 3H_2O$). ^{1}H NMR (500 MHz, DMF-d_7) δ ppm: 7.64 (d, J = 10.0 Hz, 2H), 7.98 (d, J = 10.0, 2H); ^{19}F NMR (470.4 MHz, DMF-d_7) δ ppm: −164.3 (dt, J = 4.7, 18.8 Hz, 2F), −154.5 (t, J = 18.8 Hz, 1F), −138.9 (dd, J = 4.7, 18.8 Hz, 2F); Anal. Calcd for $Rh_2(O_2CC_6H_4C_2C_6F_5)_4(Et_2O)_2\cdot 2H_2O$: C, 49.96; H, 2.60; N, 0.00%. Found: C, 49.79; H, 2.60; N, 0.13%.

Syntheses of 1-THF, 1-PN, and 1-AD. The three kinds of axial ligand substituted complexes were synthesised by the recrystallization of $Rh_2(ppeb)_4(Et_2O)_2$. $Rh_2(ppeb)_4(THF)_2$ (**1-THF**) and $Rh_2(ppeb)_4$(3-pentanone)$_2$ (**1-PN**) were obtained by the slow evaporation of the mixed solution of Et_2O/THF and Et_2O/3-pentanone containing $Rh_2(ppeb)_4(Et_2O)_2$, respectively. For $Rh_2(ppeb)_4$(1-adamantylamine)$_2$ (**1-AD**), the recrystallisation was performed by layering the Et_2O solution of 1-adamantylamine on the Et_2O solution of $Rh_2(ppeb)_4(Et_2O)_2$. FTIR-ATR (cm^{-1}): 441w, 466s, 522s, 583w, 646m, 699m, 761s, 774s, 850m, 861m, 884m, 965s, 988s, 1018w, 1042m, 1113m, 1141w, 1176w, 1286w, 1389s, 1496s, 1523m, 1549w, 1597m (COO$^-$), 2227w (C≡C), 2876w, 2978w (**1-THF**). FTIR-ATR (cm^{-1}): 411m, 465s, 522s, 582w, 645m, 699m, 725w, 761s, 774s, 813w, 849m, 859m, 964s, 989s, 1020m, 1113m, 1143w, 1178m, 1250w, 1288m, 1305m, 1391s, 1483m, 1496s, 1523m, 1548m, 1596m (COO$^-$), 1677m, 1718w, 2227w (C≡C), 2980w (**1-PN**). FTIR-ATR (cm^{-1}): 403w, 428w, 463s, 520s, 644w, 698m, 717w, 762s, 773s, 849m, 860m, 924m, 965s, 988s, 1017m, 1061w, 1094w, 1115m, 1141w, 1178w, 1290w, 1311w, 1385s, 1450w, 1496s, 1523m, 1547w, 1600m (COO$^-$), 2228w (C≡C), 2847w, 2904w, 3275w (NH_2), 3333w (NH_2) (**1-AD**).

Table 1 Crystallographic data and structural refinements for **1-THF**, **1-PN** and **1-AD**

Compound	**1-THF**	**1-PN**	**1-AD**
Formula	$C_{68}H_{32}F_{20}O_{10}Rh_2$	$C_{170}H_{132}F_{40}O_{26}Rh_4$	$C_{92}H_{70}F_{20}N_2O_{11}Rh_2$
Formula weight	1594.76	3762.40	1965.32
Temperature (°C)	−150	−150	−150
Crystal system	Monoclinic	Triclinic	Triclinic
Space group	*C*2/*m* (#12)	*P*$\bar{1}$ (#2)	*P*$\bar{1}$ (#2)
a (Å)	18.6449(7)	15.1526(7)	10.8625(8)
b (Å)	27.2267(14)	15.3844(4)	13.8827(10)
c (Å)	8.8932(4)	19.5087(4)	14.9217(11)
α (°)	90	99.0550(7)	103.6458(15)
β (°)	107.4822(12)	96.0045(7)	93.1519(15)
γ (°)	90	112.8590(7)	94.0312(16)
V (Å^3)	4306.0(3)	4069.14(17)	2175.3(3)
Z	2	1	1
D_c (g cm^{-3})	1.230	1.535	1.500
μ (mm^{-1})	0.471	0.514	0.483
F(000)	1580	1900	994
R_1 [a]	0.0660	0.0554	0.0511
wR_2 [b]	0.1742	0.1875	0.1511
Goodness-of-fit on F^2	1.135	1.111	1.089

[a] $R_1 = \sum||F_o| - |F_c||/\sum|F_o|$. [b] $wR_2 = [\sum(w(F_o^2 - F_c^2)^2)/\sum w(F_o^2)^2]^{1/2}$.

X-ray crystallography

Crystals of **1-THF**, **1-PN** and **1-AD** were mounted in a loop. Diffraction data at 123 K were measured on a RAXIS-RAPID Imaging Plate diffractometer equipped with confocal monochromated Mo-Kα radiation and data were processed using RAPID-AUTO (Rigaku). Structures were solved by direct methods and refined by full-matrix least squares techniques on F^2 (SHELXL-97).[17] All of the non-hydrogen atoms were anisotropically refined, while all of the hydrogen atoms (except for amine hydrogen atoms of 1-adamantylamine in **1-AD**, which were found on a difference Fourier map and refined isotropically) were placed geometrically and refined with a riding model with U_{iso} constrained to be 1.2 times the U_{eq} of the carrier atom. For **1-THF**, the diffused electron densities resulting from residual solvent molecules were removed from the data set using the SQUEEZE routine of PLATON and refined further using the data generated. CCDC reference numbers 1049445–1049447 (**1-THF**, **1-PN** and **1-AD**) (Table 1).

Crystal data for $Rh_2(ppeb)_4(THF)_2$ (1-THF). $C_{68}H_{32}F_{20}O_{10}Rh_2$, M_r = 1594.76, monoclinic, space group *C*2/*m*, (#12), *a* = 18.6449(7), *b* = 27.2267(14), *c* = 8.8932(4) Å, *β* = 107.4822(12)°, *V* = 4306.0(3) Å^3, *Z* = 2, *T* = 123(2) K, ρ_c = 1.230 g cm^{-3}, *μ*(Mo-Kα) = 0.471 cm^{-1}, $2\theta_{max}$ = 50.0°, *λ*(Mo-Kα) = 0.710747 Å, 16 842 reflections measured, 3892 unique (R_{int} = 0.0312), 3549 ($I > 2\sigma(I)$) were used to refine 238 parameters, 6 restraints, wR_2 = 0.1742 ($I > 2\sigma(I)$), R_1 = 0.0660 ($I > 2\sigma(I)$), GOF = 1.135.

Crystal data for $Rh_2(ppeb)_4(3\text{-pentanone})_2$ (1-PN). $C_{170}H_{132}F_{40}O_{26}Rh_4$, M_r = 3762.40, triclinic, space group *P*$\bar{1}$, (#2), *a* = 15.1526(7), *b* = 15.3844(4), *c* = 19.5087(4) Å, *α* = 99.0550(7)°, *β* = 96.0045(7)°, *γ* = 112.8590(7)°, *V* = 4069.14(17) Å^3, *Z* = 1, *T* = 123 (2) K, ρ_c = 1.535 g cm^{-3}, *μ*(Mo-Kα) = 0.514 cm^{-1}, $2\theta_{max}$ = 54.96°, *λ*(Mo-Kα) = 0.710747 Å, 40 282 reflections measured, 18 528 unique (R_{int} = 0.0223), 13 311 ($I > 2\sigma(I)$) were used to refine 1081 parameters, 0 restraints, wR_2 = 0.1875 ($I > 2\sigma(I)$), R_1 = 0.0554 ($I > 2\sigma(I)$), GOF = 1.111.

Crystal data for $Rh_2(ppeb)_4(1\text{-adamantylamine})_2$ (1-AD). $C_{92}H_{70}F_{20}N_2O_8Rh_2$, M_r = 1965.32, triclinic, space group *P*$\bar{1}$, (#2), *a* = 10.8625(8), *b* = 13.8827(10), *c* = 14.9217(11) Å, *α* = 103.6458(15)°, *β* = 93.1519(15)°, *γ* = 94.0312(16)°, *V* = 2175.3(3) Å^3, *Z* = 1, *T* = 123 (2) K, ρ_c = 1.500 g cm^{-3}, *μ*(Mo-Kα) = 0.483 cm^{-1}, $2\theta_{max}$ = 54.94°, *λ*(Mo-Kα) = 0.710747 Å, 21 333 reflections measured, 9889 unique (R_{int} = 0.031), 8336 ($I > 2\sigma(I)$) were used to refine 602 parameters, 6 restraints, wR_2 = 0.1511 ($I > 2\sigma(I)$), R_1 = 0.0511 ($I > 2\sigma(I)$), GOF = 1.089.

Results and discussion

Synthesis and characterization

Synthesis of the Rh(II) complex was performed by the reaction of $Na_4[Rh_2(CO_3)_4]\cdot 3H_2O$ with 8 eq. of Hppeb at 100 °C in DMA/H_2O (3 : 1) for 8 h. A four substituted complex, $Rh_2(ppeb)_4(Et_2O)_2$, was obtained in 27% yield by subsequent column chromatography using neutral alumina (Et_2O as the eluent). Note that the use of $Na_4[Rh_2(CO_3)_4]\cdot 3H_2O$ was crucial, and the reaction of Hppeb with carboxylate precursors, Rh(II) acetate or Rh(II) trifluoroacetate, did not afford the desired complex possibly due to the slow reaction rate of the di-substituted carboxylate complex.[15] The slow evaporation of the THF/Et_2O mixed solution of $Rh_2(ppeb)_4(Et_2O)_2$ afforded single crystals of $Rh_2(ppeb)_4(THF)_2$ (**1-THF**) suitable for X-ray crystallography. **1-PN** and **1-AD** were also obtained by recrystallization of $Rh_2(ppeb)_4(Et_2O)_2$. The recrystallisation of $Rh_2(ppeb)_4$-$(Et_2O)_2$ from slow evaporation of the mixed solution of Et_2O/3-pentanone afforded $Rh_2(ppeb)_4(3\text{-pentanone})_2$ (**1-PN**). To obtain $Rh_2(ppeb)_4(1\text{-adamantylamine})_2$ (**1-AD**), recrystallisation was performed by layering Et_2O solution of 1-adamantyl-

amine on Et_2O solution of $Rh_2(ppeb)_4(Et_2O)_2$. These three compounds were characterised by single-crystal X-ray diffraction and IR spectroscopy.

Crystal structures

The crystal structure of **1-THF** is comprised of a Rh(II) paddle-wheel with THF molecules coordinated at the axial sites (Fig. 1a). Four $ppeb^-$ ligands occupied the positions in the equatorial plane of each rhodium atom. The Rh1–Rh1′ distance was 2.3875(13) Å, which is in the range found for previously reported Rh(II) paddle-wheel dimers (2.316 to 2.486 Å).[18] The angle between the phenylene and perfluorophenyl rings was estimated to be 18.4°.

In the crystal packing structure of **1-THF**, the aforementioned multipoint Ar–Ar^F interaction played a key role in stabilising the molecular assembly. As shown in Fig. 1b, an infinite two-dimensional (2-D) square-grid sheet structure was formed *via* multipoint Ar–Ar^F interactions between the ligands. The mean interplanar separation between the phenylene and perfluorophenyl rings was 3.56(16) Å. These 2-D sheets were stacked through π–π interactions (denoted as blue line in Fig. 1b) to form a columnar structure of paddle-wheel units along the *c* axis. As a result, a porous structure with the channel entrance size[19] of 13.8 × 12.1 $Å^2$ was formed (Fig. 1c), and THF molecules were contained in the pores as guests. The recrystallisation of $Rh_2(ppeb)_4(Et_2O)_2$ from Et_2O/3-pentanone afforded a similar crystal structure composed of a Rh(II) paddle-wheel complex bearing 3-pentanone at the axial sites, $Rh_2(ppeb)_4$(3-pentanone)$_2$ (**1-PN**) (Fig. 2a). In the crystal struc-

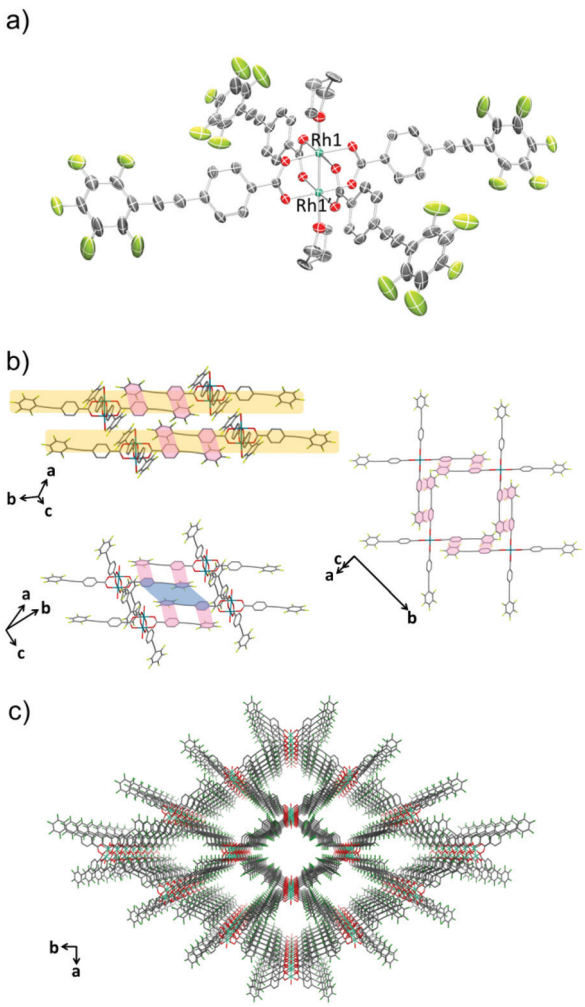

Fig. 1 (a) An ORTEP drawing of **1-THF** (50% probability ellipsoids). Hydrogen atoms are omitted for clarity. (b) 2-D sheet structure of **1-THF**. Ar–Ar^F interactions and π–π interactions are shown in red and blue lines respectively. Hydrogen atoms and carbon atoms of THF at the axial positions are omitted for clarity. (c) Crystal packing of **1-THF** along the *c* axis. Hydrogen atoms, and carbon atoms of THF at the axial positions are omitted for clarity. O = red, C = grey, F = pale green, Rh = sea green.

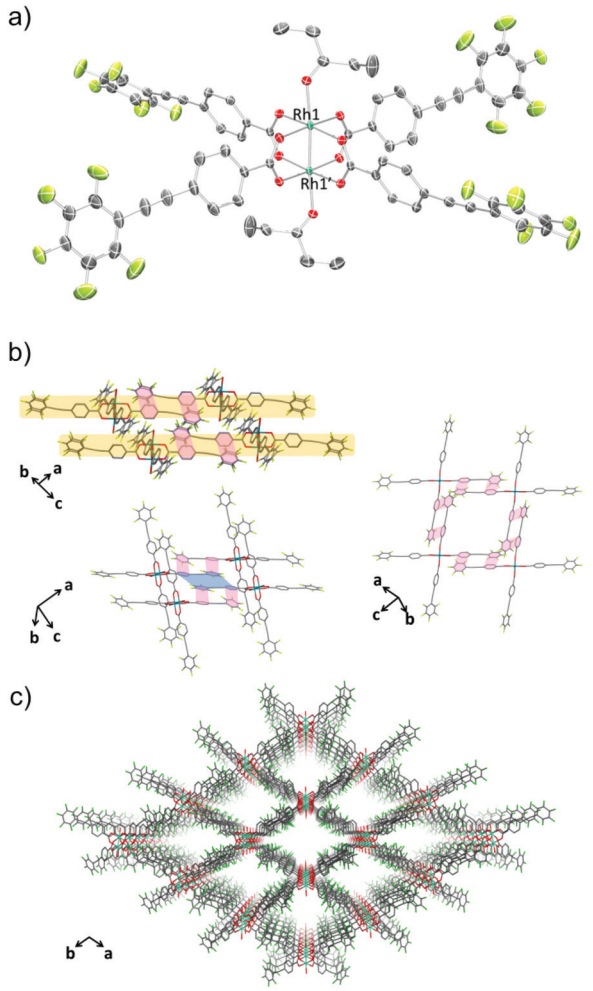

Fig. 2 (a) An ORTEP drawing of **1-PN** (50% probability ellipsoids). Hydrogen atoms and crystal solvent molecules are omitted for clarity. (b) 2-D sheet structure of **1-PN**. Ar–Ar^F interactions and π–π interactions are shown in red and blue lines respectively. Hydrogen atoms, carbon atoms of 3-pentanone at the axial positions and crystal solvent molecules observed in the channels are omitted for clarity. (c) Crystal packing of **1-PN** along the *c* axis. Hydrogen atoms, and carbon atoms of 3-pentanone at the axial positions and crystal solvent molecules observed in the channels are omitted for clarity. O = red, C = grey, F = pale green, Rh = sea green.

ture of **1-PN**, the mean interplanar separation between phenylene and perfluorophenyl rings was 3.49(12) Å, and the channel entrance size was estimated to be 12.9 × 10.5 Å^2. It should be noted that the active sites of these complexes were exposed to the pores in both structures.

The reaction of $Rh_2(ppeb)_4(Et_2O)_2$ with 1-adamantylamine was subsequently performed to examine the adjustability of the framework to bulky molecules, and the targeted axial ligand substituted complex, $Rh_2(ppeb)_4$(1-adamantylamine)$_2$ (**1-AD**, Fig. 3a), was obtained. The distance between two rhodium atoms in **1-AD** was 2.4140(7) Å, which is comparable to that of **1-THF** or **1-PN**. For **1-AD**, the angles between the phenylene and perfluorophenyl rings were 16.3° and 5.9°. In the crystal structure of **1-AD**, a 2-D sheet structure stabilised by multipoint Ar–Ar^F interactions was also obtained (Fig. 3b). However, π–π interactions between the 2-D sheets were not observed because the bulkiness of the axial ligands prevented a close contact between sheets. Alternatively, the ppeb$^-$ ligands exhibited a conformation almost perpendicular to the 2-D sheets, and CF–π interactions[20] between the ppeb$^-$ ligands formed inter-sheet stacking. As a result, a 1-D channel structure with an entrance size of 10.1 × 8.2 Å^2 was obtained (Fig. 3c). The mean interplanar separation between the phenylene and perfluorophenyl rings was 3.50(16) Å. The axial ligands were also exposed to the pores despite the different stacking mode from **1-THF** and **1-PN**. The comparison between the assembling-patterns between these structures is shown in Fig. 4. The horizontal distances between the Rh dimeric nodes in neighbouring 2-D sheets (denoted as d_1 and d_2) were found to be $d_1 = d_2 = 4.96$ Å for **1-THF**, $d_1 = 6.08$ Å, $d_2 = 5.82$ Å for **1-PN** and $d_1 = 10.70$ Å, $d_2 = 6.11$ Å for **1-AD** and were mainly different between the three structures, reflecting the bulkiness of the axial ligands. These crystallographic observations indicate that the 2-D sheet structures in these porous frameworks are well defined by the multipoint Ar–Ar^F interactions and that the interlayer stacking structures are controllable in response to the size and shape of the axial ligands.

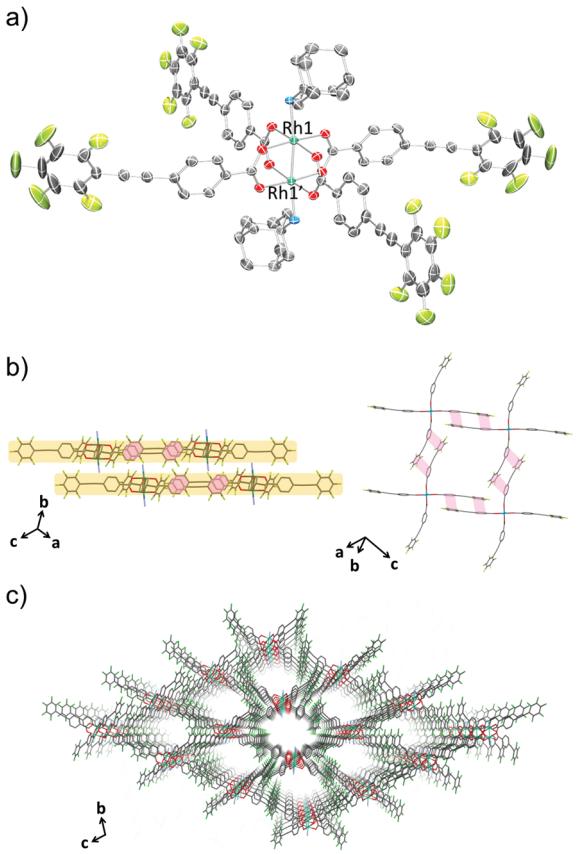

Fig. 3 (a) An ORTEP drawing of **1-AD** (50% probability ellipsoids). Hydrogen atoms and crystal solvent molecules are omitted for clarity. (b) 2-D sheet structure of **1-AD**. Ar–Ar^F interactions are shown in red lines. Hydrogen atoms, and carbon atoms of 1-adamantylamine at the axial positions and crystal solvent molecules observed in the channels are omitted for clarity. (c) Crystal packing of **1-AD** along the *a* axis. Hydrogen atoms, and carbon atoms of 1-adamantylamine at the axial positions and crystal solvent molecules observed in the channels are omitted for clarity. O = red, C = grey, F = pale green, N = blue, Rh = sea green.

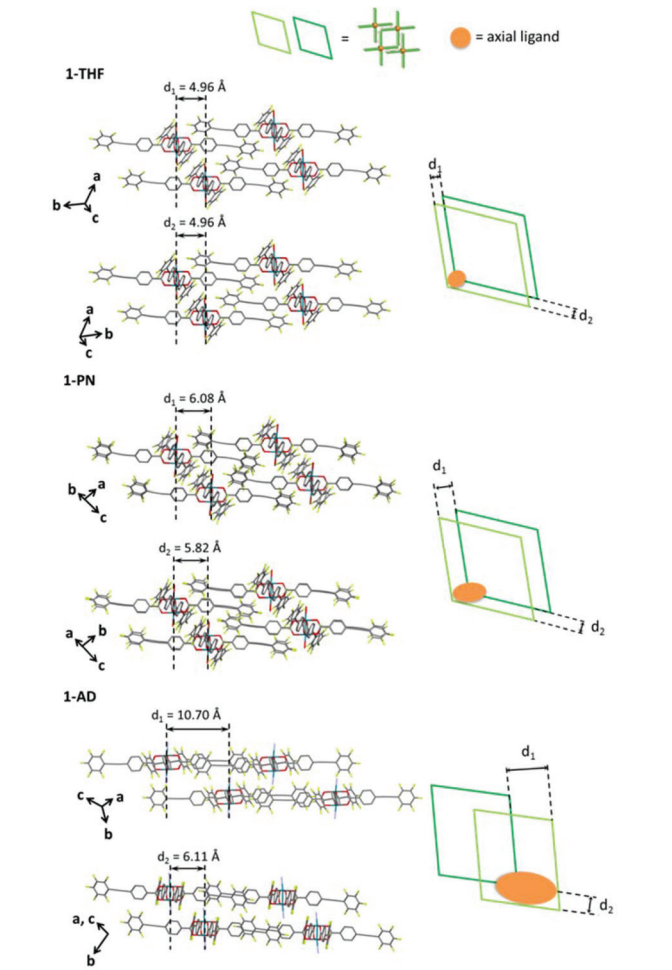

Fig. 4 Side view of the crystal packing (left) and the schematic illustration of the top view of the interlayer stacking structure (right) for **1-THF** (top), **1-PN** (middle) and **1-AD** (bottom). In the schematic illustration, the axial ligands are represented as orange circles.

The effect of the axial ligands on the porous properties

The effect of the axial ligands on the porous properties of the frameworks was also investigated by several measurements. A TG curve of **1-AD** exhibited no weight loss upon heating up to 284 °C (Fig. 5c), which indicated the strong coordination ability of the axial ligands to the metal centres. Upon further heating up to 600 °C, the degradation of the complex was observed. It should be noted that the removal of the guest molecules (Et_2O) was not observed due to their highly volatile nature. The removal of the axial ligand was also not observed due to their strong coordination ability. Furthermore, the CO_2 adsorption isotherms for **1-AD** evacuated at 40 °C (Fig. 5f) and 120 °C (Fig. S1c in the ESI†) exhibited almost identical sorption profiles, suggesting the retention of the porous structure due to the "capping" of the active sites with the strongly coordinated axial ligands. In contrast, the TG curves of **1-THF** and **1-PN** indicated the release of the axial ligands in the temperature range of 100–170 °C with a weight loss of 5.30% (**1-THF**) and 5.82% (**1-PN**), respectively (Fig. 5a and b). The degradation of the complexes was observed in the temperature range of 327–600 °C. In the CO_2 adsorption isotherms of **1-THF** and **1-PN** evacuated at 40 °C and 120 °C, the amount of adsorbed CO_2 gradually increased as the pressure increased and showed hysteresis during the desorption process (Fig. 5d and e and Fig. S1a and b in the ESI†) and the adsorption amount is dependent on the temperature of pre-treatment, which may be attributed to the transformation of the interlayer stacking structure arising from the exchange or the loss of the axial ligands. These results clearly indicate the difference in the lability of the axial ligands between **1-AD** and other two structures, **1-THF** and **1-PN**. Additionally, N_2 adsorption measurements at 77 and 195 K were performed and almost no adsorption of N_2 was observed for **1-THF** and **1-PN** (Fig. S2a and b, and Fig. S3a and b in the ESI†), suggesting the selective CO_2 adsorption over N_2 in these frameworks. In contrast to **1-THF** and **1-PN**, N_2 was slightly adsorbed to **1-AD** at 77 K (Fig. S2c in the ESI†), although no adsorption of N_2 was observed at 195 K (Fig. S3c in the ESI†).

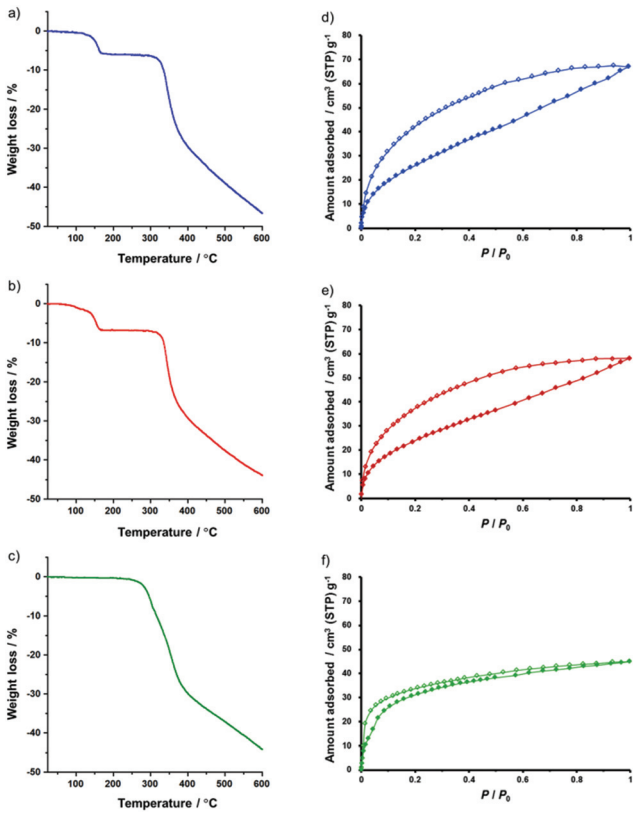

Fig. 5 TGA profiles of (a) **1-THF**, (b) **1-PN** and (c) **1-AD** with a heating rate of 20 K min^{-1}. CO_2 sorption isotherms of (d) **1-THF**, (e) **1-PN** and (f) **1-AD** at 195 K. Filled shapes: adsorption. Open shapes: desorption. The samples of **1-THF**, **1-PN** and **1-AD** for the CO_2 adsorption were evacuated at 40 °C before the measurements.

PXRD measurements of the samples after the removal of the guest molecules and the dissociation of the axial ligands were performed to investigate the structural change in these processes. The experiments were performed for **1-AD** and **1-PN**, which have the unremovable axial ligands and the removable ligands, respectively. Note that the PXRD patterns for the as-synthesized compounds were measured under the vapour of the guest molecules to prevent the loss of the guest molecules. In the case of **1-AD**, the PXRD pattern changed after the evacuation at 40 °C (from A to B in Fig. S4 in the ESI†), suggesting the structural change attributed to the removal of the guest molecules. Subsequent evacuation of the sample at 120 °C gave the almost identical PXRD pattern (Fig. S4C in the ESI†), which indicates the strong coordination of axial ligands. These results are fully consistent with the result of TGA and CO_2 adsorption measurements. In the case of **1-PN**, the PXRD pattern changed after evacuation at 40 °C (from D to E in Fig. S5 in the ESI†) and the structural transformation accompanied by the removal of the guest molecules was observed. In contrast to **1-AD**, the subsequent evacuation at 120 °C caused the significant change of the PXRD pattern (from E to F in Fig. S5 in the ESI†) and the structural transformation due to the dissociation of the axial ligands was indicated. At this stage, we could not determine the structure after the removal of the guest molecules or the axial ligands, and thus, the detailed discussion on the CO_2 adsorption profiles was not allowed. However, the results of CO_2 adsorption and PXRD measurements revealed that the crystallinity and porosity of the sample were maintained throughout the removal of the guest molecules and the dissociation of the axial ligands, and the framework structures transformed flexibly accompanied by these processes.

Additionally, the PXRD patterns before and after the CO_2 adsorption were also examined. As shown in Fig. S6–9, in the ESI,† the samples of **1-PN** and **1-AD** did not show significant change in the PXRD pattern after the CO_2 adsorption measurements regardless of the pre-treatment temperature. These results indicate that our frameworks recover their initial structures after the CO_2 adsorption/desorption processes.

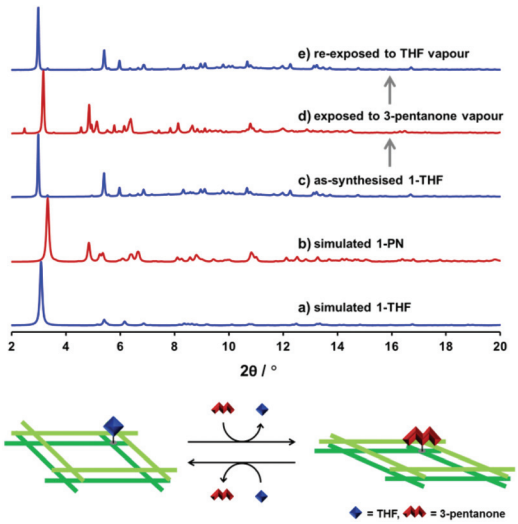

Fig. 6 Simulated XRD patterns of (a) **1-THF** and (b) **1-PN** and PXRD patterns of as-synthesised (c) **1-THF**, (d) the sample of **1-THF** exposed to 3-pentanone vapour, and (e) the sample re-exposed to THF vapour. Schematic illustration of the structural transformation between **1-THF** and **1-PN** induced by the reversible ligand substitution reaction (bottom) (λ = 0.79978 Å).

Flexible structural transformation during the ligand exchange reaction of the frameworks

The structural flexibility of **1-THF** and **1-PN** and the reactivity of the open axial sites in these frameworks were examined by PXRD measurements. Initially, a crystalline sample of **1-THF** was evacuated at room temperature for 1 h and exposed to 3-pentanone vapour for 1 h. PXRD patterns before and after the treatment suggested the complete structural transformation from **1-THF** to **1-PN** (Fig. 6c and d, blue and red lines). Subsequently, the obtained powder sample of **1-PN** was evacuated at room temperature for 1 h and exposed to THF vapour for 1 h. The PXRD pattern of the sample treated with THF revealed the regeneration of **1-THF** (Fig. 6e). These results indicate that the active sites of the SBUs in our framework effectively worked to control the structural flexibility of each phase.

Conclusions

In conclusion, we demonstrated the construction and structural determination of porous frameworks composed of a substitution-inert complex with active sites. Three novel Rh(II) paddle-wheel complexes, $Rh_2(ppeb)_4(X)_2$ (X = THF (**1-THF**), 3-pentanone (**1-PN**), and 1-adamantylamine (**1-AD**)), were successfully assembled to form porous frameworks with a solvent accessible columnar channel by utilizing the multipoint $Ar–Ar^F$ interaction. The obtained supramolecular structures possessed active sites exposed to the channel, and the comparison of crystal packing of the three complexes revealed the structural difference induced by the size and the structure of the axial ligands. Furthermore, the porous properties of these frameworks were also examined by several experiments. Although the axial ligands of **1-AD** did not dissociate upon heating and during the sorption process, the axial ligands of **1-THF** and **1-PN** were labile to the axial ligand substitution reaction, and the induced-fit structural transformation in response to the ligand substitution was observed in the crystalline state. We believe that our results presented here should be a key example to construct porous materials based on substitution-inert metal ions with active sites that can be applied for catalytic reactions and chemical sensors.

Acknowledgements

This work was supported by a Grant-in-Aid for Young Scientists (A) (No. 15H05480) (to M.K.), a Grant-in-Aid for Young Scientists (A) (No. 25708011) (to S.M.), a Grant-in-Aid for Challenging Exploratory Research (No. 26620160) (to S.M.), and a Grant-in-Aid for JSPS Fellows (No. K2S2605890) (to T.I.) from the Japan Society for the Promotion of Science. This work was also supported by a Grant-in-Aid for Scientific Research on Innovative Areas "AnApple" (No. 15H00889). The synchrotron radiation experiments were performed at the BL02B2 of SPring-8 with the approval of the Japan Synchrotron Radiation Research Institute (JASRI) (Proposal No. 2014B1428).

Notes and references

1 (*a*) B. Moulton and M. J. Zaworotko, *Chem. Rev.*, 2001, **101**, 1629–1658; (*b*) S. Kitagawa, R. Kitaura and S. Noro, *Angew. Chem., Int. Ed.*, 2004, **43**, 2334–2375; (*c*) G. Férey and C. Serre, *Chem. Soc. Rev.*, 2009, **38**, 1380–1399; (*d*) J. Lee, O. K. Farha, J. Roberts, K. A. Scheidt, S. T. Nguyen and J. T. Hupp, *Chem. Soc. Rev.*, 2009, **38**, 1450–1459; (*e*) M. D. Allendorf, C. A. Bauer, R. K. Bhakta and R. J. T. Houk, *Chem. Soc. Rev.*, 2009, **38**, 1330–1352; (*f*) D. Zacher, O. Shekhah, C. Wöll and R. A. Fischer, *Chem. Soc. Rev.*, 2009, **38**, 1418–1429; (*g*) K. Sumida, D. L. Rogow, J. A. Mason, T. M. McDonald, E. D. Bloch, Z. R. Herm, T.-H. Bae and J. R. Long, *Chem. Rev.*, 2012, **112**, 724–781; (*h*) M. Yoon, R. Srirambalaji and K. Kim, *Chem. Rev.*, 2012, **112**, 1196–1231; (*i*) J.-R. Li, J. Sculley and H.-C. Zhou, *Chem. Rev.*, 2012, **112**, 869–932; (*j*) C. Wang, T. Zhang and W. Lin, *Chem. Rev.*, 2012, **112**, 1084–1104; (*k*) H. Furukawa, K. E. Cordova, M. O'Keeffe and O. M. Yaghi, *Science*, 2013, **341**, 974–986.

2 (*a*) Y. Inokuma, S. Yoshioka, J. Ariyoshi, T. Arai, Y. Hitora, K. Takada, S. Matsunaga, K. Rissanen and M. Fujita, *Nature*, 2013, **495**, 461–466; (*b*) B. D. Chandler, G. D. Enright, K. A. Udachin, S. Pawsey, J. A. Ripmeester, D. T. Cramb and G. K. H. Shimizu, *Nat. Mater.*, 2008, **7**, 229–235; (*c*) W. M. Bloch, A. Burgun, C. J. Coghlan, R. Lee, M. L. Coote, C. J. Doonan and C. J. Sumby, *Nat. Chem.*, 2014, **6**, 906–912; (*d*) J. Rabone, Y.-F. Yue, S. Y. Chong, K. C. Stylianou, J. Bacsa, D. Bradshaw, G. R. Darling,

N. G. Berry, Y. Z. Khimyak, A. Y. Ganin, P. Wiper, J. B. Claridge and M. J. Rosseinsky, *Science*, 2010, **329**, 1053–1057; (*e*) G. K. H. Shimizu, J. M. Taylor and S. Kim, *Science*, 2013, **341**, 354–355; (*f*) H. Deng, S. Grunder, K. E. Cordova, C. Valente, H. Furukawa, M. Hmadeh, F. Gándara, A. C. Whalley, Z. Liu, S. Asahina, H. Kazumori, M. O'Keeffe, O. Terasaki, J. F. Stoddart and O. M. Yaghi, *Science*, 2012, **336**, 1018–1023.

3 (*a*) E. D. Bloch, W. L. Queen, R. Krishna, J. M. Zadrozny, C. M. Brown and J. R. Long, *Science*, 2012, **335**, 1606–1610; (*b*) S. Xiang, Z. Zhang, C. Zhao, K. Hong, X. Zhao, D. Ding, M. Xie, C. Wu, M. C. Das, R. Gill, K. M. Thomas and B. Chen, *Nat. Commun.*, 2011, **2**, 204; (*c*) E. D. Bloch, M. R. Hudson, J. A. Mason, S. Chavan, V. Crocellà, J. D. Howe, K. Lee, A. L. Dzubak, W. L. Queen, J. M. Zadrozny, S. J. Geier, L.-C. Lin, L. Gagliardi, B. Smit, J. B. Neaton, S. Bordiga, C. M. Brown and J. R. Long, *J. Am. Chem. Soc.*, 2014, **136**, 10752–10761; (*d*) Y.-S. Bae, C. Y. Lee, K. C. Kim, O. K. Farha, P. Nickias, J. T. Hupp, S. T. Nguyen and R. Q. Snurr, *Angew. Chem., Int. Ed.*, 2012, **51**, 1857–1860; (*e*) Z. Guo, H. Wu, G. Srinivas, Y. Zhou, S. Xiang, Z. Chen, Y. Yang, W. Zhou, M. O'Keeffe and B. Chen, *Angew. Chem., Int. Ed.*, 2011, **50**, 3178–3181.

4 (*a*) C.-D. Wu, A. Hu, L. Zhang and W. Lin, *J. Am. Chem. Soc.*, 2005, **127**, 8940–8941; (*b*) Z. Zhang, Y. Chen, S. He, J. Zhang, X. Xu, Y. Yang, F. Nosheen, F. Saleem, W. He and X. Wang, *Angew. Chem., Int. Ed.*, 2014, **53**, 12517–12521; (*c*) W. Xuan, C. Ye, M. Zhang, Z. Chen and Y. Cui, *Chem. Sci.*, 2013, **4**, 3154–3159.

5 (*a*) B. Chen, Y. Yang, F. Zapata, G. Lin, G. Qian and E. B. Lobkovsky, *Adv. Mater.*, 2007, **19**, 1693–1696; (*b*) N. B. Shustova, A. F. Cozzolino, S. Reineke, M. Baldo and M. Dincă, *J. Am. Chem. Soc.*, 2013, **135**, 13326–13329.

6 (*a*) S. S.-Y. Chui, S. M.-F. Lo, J. P. H. Charmant, A. G. Orpen and I. D. Williams, *Science*, 1999, **283**, 1148–1150; (*b*) N. L. Rosi, J. Kim, M. Eddaoudi, B. Chen, M. O'Keeffe and O. M. Yaghi, *J. Am. Chem. Soc.*, 2005, **127**, 1504–1518.

7 (*a*) P. Ceccherelli, M. Curini, M. C. Marcotullio and O. Rosati, *Tetrahedron*, 1991, **47**, 7403–7408; (*b*) M. P. Doyle, *Acc. Chem. Res.*, 1986, **19**, 348–356; (*c*) M. P. Doyle, K. G. High, C. L. Neslonely, T. W. Clayton Jr. and J. Lin, *Organometallics*, 1991, **10**, 1225–1226; (*d*) S. Tanaka, S. Masaoka, K. Yamauchi, M. Annaka and K. Sakai, *Dalton Trans.*, 2010, **39**, 11218–11226; (*e*) D. K. Kumar, A. S. Filatov, M. Napier, J. Sun, E. V. Dikarev and M. A. Petrukhina, *Inorg. Chem.*, 2012, **51**, 4855–4861; (*f*) J. Hansen and H. M. L. Davies, *Coord. Chem. Rev.*, 2008, **252**, 545–555; (*g*) K. P. Kornecki, J. F. Briones, V. Boyarskikh, F. Fullilove, J. Autschbach, K. E. Schrote, K. M. Lancaster, H. M. L. Davies and J. F. Berry, *Science*, 2013, **342**, 351–354.

8 (*a*) G. Férey, C. Serre, C. Mellot-Draznieks, F. Millange, S. Surblé, J. Dutour and I. Margiolaki, *Angew. Chem., Int. Ed.*, 2004, **43**, 6296–6301; (*b*) G. Férey, C. Mellot-Draznieks, C. Serre, F. Millange, S. Surblé, J. Dutour and I. Margiolaki, *Science*, 2005, **309**, 2040–2042.

9 (*a*) P. D. C. Dietzel, Y. Morita, R. Blom and H. Fjellvåg, *Angew. Chem., Int. Ed.*, 2005, **44**, 6354–6358; (*b*) B. Chen, N. W. Ockwig, A. R. Millward, D. S. Contreras and O. M. Yaghi, *Angew. Chem., Int. Ed.*, 2005, **44**, 4745–4749; (*c*) X.-S. Wang, S. Ma, P. M. Forster, D. Yuan, J. Eckert, J. J. López, B. J. Murphy, J. B. Parise and H.-C. Zhou, *Angew. Chem., Int. Ed.*, 2008, **47**, 7263–7266; (*d*) D. Yuan, D. Zhao, D. Sun and H.-C. Zhou, *Angew. Chem., Int. Ed.*, 2010, **49**, 5357–5361; (*e*) M. Dincă, A. Dailly, Y. Liu, C. M. Brown, D. A. Neumann and J. R. Long, *J. Am. Chem. Soc.*, 2006, **128**, 16876–16883; (*f*) T. M. McDonald, D. M. D'Alessandro, R. Krishnac and J. R. Long, *Chem. Sci.*, 2011, **2**, 2022–2028; (*g*) Y. Liu, J. F. Eubank, A. J. Cairns, J. Eckert, V. C. Kravtsov, R. Luebke and M. Eddaoudi, *Angew. Chem., Int. Ed.*, 2007, **46**, 3278–3283; (*h*) M. Pang, A. J. Cairns, Y. Liu, Y. Belmabkhout, H. C. Zeng and M. Eddaoudi, *J. Am. Chem. Soc.*, 2012, **134**, 13176–13179.

10 (*a*) P. Li, Y. He, J. Guang, L. Weng, J. C.-G. Zhao, S. Xiang and B. Chen, *J. Am. Chem. Soc.*, 2014, **136**, 547–549; (*b*) W. Yang, A. Greenaway, X. Lin, R. Matsuda, A. J. Blake, C. Wilson, W. Lewis, P. Hubberstey, S. Kitagawa, N. R. Champness and M. Schröder, *J. Am. Chem. Soc.*, 2010, **132**, 14457–14469; (*c*) M. Mastalerz and I. M. Oppel, *Angew. Chem., Int. Ed.*, 2012, **51**, 5252–5255; (*d*) S. A. Dalrymple and G. K. H. Shimizu, *J. Am. Chem. Soc.*, 2007, **129**, 12114–12116; (*e*) P. S. Nugent, V. L. Rhodus, T. Pham, K. Forrest, L. Wojtas, B. Space and M. J. Zaworotko, *J. Am. Chem. Soc.*, 2013, **135**, 10950–10953; (*f*) P. Li, Y. He, Y. Zhao, L. Weng, H. Wang, R. Krishna, H. Wu, W. Zhou, M. O'Keeffe, Y. Han and B. Chen, *Angew. Chem., Int. Ed.*, 2015, **54**, 574–577.

11 (*a*) M. J. Bojdys, M. E. Briggs, J. T. A. Jones, D. J. Adams, S. Y. Chong, M. Schmidtmann and A. I. Cooper, *J. Am. Chem. Soc.*, 2011, **133**, 16566–16571; (*b*) T. Kaczorowski, I. Justyniak, T. Lipińska, J. Lipkowski and J. Lewiński, *J. Am. Chem. Soc.*, 2009, **131**, 5393–5395; (*c*) M. Mastalerz, M. W. Schneider, I. M. Oppel and O. Presly, *Angew. Chem., Int. Ed.*, 2011, **50**, 1046–1051; (*d*) K. Sokołowski, W. Bury, I. Justyniak, D. Fairen-Jimenez, K. Sołtys, D. Prochowicz, S. Yang, M. Schröder and J. Lewiński, *Angew. Chem., Int. Ed.*, 2013, **52**, 13414–13418; (*e*) G. Zhang, O. Presly, F. White, I. M. Oppel and M. Mastalerz, *Angew. Chem., Int. Ed.*, 2014, **53**, 1516–1520; (*f*) C. Redshaw, S. Jana, C. Shang, M. R. J. Elsegood, X. Lu and Z. X. Guo, *Organometallics*, 2010, **29**, 6129–6132.

12 (*a*) J. Lü, C. Perez-Krap, M. Suyetin, N. H. Alsmail, Y. Yan, S. Yang, W. Lewis, E. Bichoutskaia, C. C. Tang, A. J. Blake, R. Cao and M. Schröder, *J. Am. Chem. Soc.*, 2014, **136**, 12828–12831; (*b*) W. Bury, I. Justyniak, D. Prochowicz, A. Rola-Noworyta and J. Lewiński, *Inorg. Chem.*, 2012, **51**, 7410–7414; (*c*) J. Lewiński, T. Kaczorowski, D. Prochowicz, T. Lipińska, I. Justyniak, Z. Kaszkur and J. Lipkowski, *Angew. Chem., Int. Ed.*, 2010, **49**, 7035–7039.

13 (*a*) H. Kim, Y. Kim, M. Yoon, S. Lim, S. M. Park, G. Seo and K. Kim, *J. Am. Chem. Soc.*, 2010, **132**, 12200–12202; (*b*) T. Tozawa, J. T. A. Jones, S. I. Swamy, S. Jiang, D. J. Adams, S. Shakespeare, R. Clowes, D. Bradshaw,

T. Hasell, S. Y. Chong, C. Tang, S. Thompson, J. Parker, A. Trewin, J. Bacsa, A. M. Z. Slawin, A. Steiner and A. I. Cooper, *Nat. Mater.*, 2009, **8**, 973–978; (*c*) J. T. A. Jones, T. Hasell, X. Wu, J. Bacsa, K. E. Jelfs, M. Schmidtmann, S. Y. Chong, D. J. Adams, A. Trewin, F. Schiffman, F. Cora, B. Slater, A. Steiner, G. M. Day and A. I. Cooper, *Nature*, 2011, **474**, 367–371; (*d*) C. G. Bezzu, M. Helliwell, J. E. Warren, D. R. Allan and N. B. McKeown, *Science*, 2010, **327**, 1627–1630; (*e*) T. Hasell, S. Y. Chong, M. Schmidtmann, D. J. Adams and A. I. Cooper, *Angew. Chem., Int. Ed.*, 2012, **51**, 7154–7157; (*f*) M. W. Schneider, I. M. Oppel, A. Griffin and M. Mastalerz, *Angew. Chem., Int. Ed.*, 2013, **52**, 3611–3615.

14 (*a*) J. H. Williams, *Acc. Chem. Res.*, 1993, **26**, 593–598; (*b*) C. R. Patrick and G. S. Prosser, *Nature*, 1960, **187**, 1021.

15 T. Itoh, M. Kondo, M. Kanaike and S. Masaoka, *CrystEngComm*, 2013, **15**, 6122–6126.

16 C. R. Willson and H. Taube, *Inorg. Chem.*, 1975, **47**, 533–535.

17 G. M. Sheldrick, *Program for Crystal Structure Refinement*, University of Göttingen, Germany, 1997.

18 (*a*) F. A. Cotton, C. A. Murillo and R. A. Walton, "*Multiple Bonds Between Metal Atoms*", Springer Science and Business Media, New York, 3rd edn, 2005; (*b*) E. B. Royar and S. D. Robinson, *Platinum Metals Rev.*, 1982, **26**, 65–69.

19 The channel entrance size was estimated by considering the van der Waals radii of constituent atoms, and the atoms at axial ligands are omitted for the calculation.

20 (*a*) N. Hayashi, T. Mori and K. Matsumoto, *Chem. Commun.*, 1998, 1905–1906; (*b*) K. Reichenbächer, H. I. Süss and J. Hulliger, *Chem. Soc. Rev.*, 2005, **34**, 22–30; (*c*) X. Xu, B. Pooi, H. Hirao and S. H. Hong, *Angew. Chem., Int. Ed.*, 2014, **53**, 1283–1287.